

Reaction Mechanisms of IO Radical Formation from the Reaction of CH_3I with Cl Atom in the Presence of O_2

Shinichi Enami,[1,†] Yosuke Sakamoto,[1] Takashi Yamanaka,[1] Satoshi Hashimoto,[1] Masahiro Kawasaki,*[1] Kenichi Tonokura,[2] and Hiroto Tachikawa[3]

[1]Department of Molecular Engineering, Kyoto University, Kyotodaigaku-Katsura, Nishikyo-ku, Kyoto 615-8510

[2]Environmental Science Center, The University of Tokyo, 7-3-1 Hongo, Bunkyo-ku, Tokyo 113-0033

[3]Department of Materials Chemistry, Faculty of Engineering, Hokkaido University, N13 W8, Kita-ku, Sapporo 060-8628

Received April 8, 2008; E-mail: kawasaki@moleng.kyoto-u.ac.jp

The yields of IO radical from the reaction of CH_3I with Cl atom in the presence of O_2 were determined as functions of total pressure from 5 to 250 Torr of N_2 diluent and temperature over the range of 278 to 328 K using cavity ring-down spectroscopy. The yields are pressure and temperature dependent. The rate constants and product branching ratios of the reaction of CH_2I radical with O_2 were investigated. We determined a rate constant of $(1.28 \pm 0.22) \times 10^{-12}$ $cm^3\,molecule^{-1}\,s^{-1}$ at 298 K (2σ uncertainty) for this reaction. Theoretical calculations were performed to determine energetics of the reactions of $CH_2I + O_2$ and $CH_2Br + O_2$. The present results suggest that non-negligible IO radicals will be formed from the reactions of $CH_3I/CH_2I_2 + OH/Cl/NO_3$ at atmospheric conditions.

Tropospheric iodine chemistry has attracted great attention because of its significant effect on ozone depletion[1–5] and the new particle formation.[6–8] Under conditions typical for the tropical marine environment, iodine chemistry is responsible for around 6% of total tropospheric column ozone destruction, and in marine regions of high marine biological activity this value could reach 30%.[9] Fine sea salt aerosol particles containing iodide, which is 100–1000 times concentrated compared with seawater, react with gaseous ozone and may globally release photoactive inorganic halogen compounds, e.g. Br_2, into the atmosphere.[10] Thus, iodine compounds play various and significant roles in tropospheric chemistry and the iodine chemistry now becomes to be the most interesting topics.[1]

The main source of gaseous iodine compounds in the marine boundary layer is suggested to be biogenic emission of alkyl iodides and inorganic iodine.[1,4] Recent reports show that brown algae of the Laminariales (kelps) are the strongest accumulators of iodine among living organisms and these kelps under oxidative stress releases iodine species.[11,12] An extraordinarily high concentration of CH_3I, 1830 pptv, was recently measured at the French Atlantic Coast.[13] Although the major fate of marine boundary layer CH_3I will be photodissociation to CH_3 and I, H-atom abstraction by OH radicals and Cl atoms will account for around 10 to 20% of the CH_3I loss in the troposphere.[1] The maximum predicted levels of Cl atoms occur shortly after sunrise, peaking at 10^5 atom cm^{-3}, while the OH mixing ratio is 4×10^5 molecule cm^{-3}.[14] Hence, in coastal areas, the reaction with Cl is expected to be appreciable.[15]

$$CH_3I + OH/Cl \rightarrow CH_2I + H_2O/HCl \quad (1)$$

The atmospheric fate of CH_2I radical has been considered to be the formation of its peroxy radical.[16]

$$CH_2I + O_2 + M \rightarrow CH_2IO_2 + M \quad (2a)$$

We had previously reported the formation of IO via reaction (2b).[17]

$$CH_2I + O_2 \rightarrow IO + HCHO \quad (2b)$$

The formation of the IO radical was reported during the reaction of iodoalkyl radicals (RCHI), where R stands for C_nH_{2n+1} ($n = 1$–3), or *cyclo*-$C_6H_{10}I$ radical with O_2 at 298 K.[18] Recently, unexpected high concentrated IO radical was observed in the west coast of France[19] and in coastal Antarctica.[20] Nighttime observation of IO radical and OIO radical at Mace Head was also reported by Saiz-Lopez, Plane, and co-worker[21] suggesting the reaction $I_2 + NO_3$ to be a possible source of atomic iodine that subsequently reacts with O_3 to form IO.[21] Recent laboratory studies show that CH_3I/CH_2I_2 react rapidly with NO_3 and likely produce CH_2I/CHI_2 radical.[22,23]

$$CH_3I + NO_3 \rightarrow CH_2I + HNO_3 \quad (3)$$

$$CH_2I_2 + NO_3 \rightarrow CHI_2 + HNO_3 \quad (4)$$

These processes may also play a role in nighttime halogen cycles if CH_2I/CHI_2 radical is efficiently converted to the IO radical via reaction 2b.

Recently, Stefanopoulos et al.[24] reported that the primary products from the reaction of $CH_2I/CHI_2 + O_2$ are HCHO and HCOOH using the combination of a Knudsen reactor, electron-impact mass spectrometry and FT-IR, which implies that IO radical and I atom formations are main channels in these reactions.

In this paper we report the reaction rate constant and the IO radical yields from reaction 2 using cavity ring-down spectroscopy (CRDS).[25–27] The photodissociation of Cl_2 at 355 nm

† Present address: W. M. Keck Laboratories, California Institute of Technology, Pasadena, CA 91125, USA

Published on the web October 10, 2008; doi:10.1246/bcsj.81.1250

generates Cl atom which abstracts an H-atom from CH_3I to produce CH_2I radical. Theoretical calculations on $CH_2I + O_2$ reaction energetics support the direct formation of IO radical from reaction 2b.

Experimental

The CRDS apparatus used in the present study has been described in detail elsewhere.[28] The cavity ring-down mirrors (Research Electro-Optics, 7.8 mm dia. and 1 m curvature) had a specified maximum reflectivity of 0.9994 and were mounted 1.04 m apart. Light leaking from the end mirror was detected by a photomultiplier tube (Hamamatsu Photonics, R212UH) through a band pass filter. The ring-down signal of the light intensity was sampled by a digitizing oscilloscope (Tektronix, TDS-714L, 500 MHz, 500 MS/s, 8-bit resolution) and recorded in a personal computer. The decay of the light intensity is represented by eq 5;

$$I(t) = I_0 \exp(-t/\tau) = I_0 \exp(-t/\tau_0 - \sigma N c L_R t/L) \quad (5)$$

where I_0 and $I(t)$ are the light intensities at time 0 and t, respectively. τ_0 is the cavity ring-down time without photolysis laser light (about 5 μs at 440 nm), L_R the length of the reaction region (0.47 ± 0.01 m), L the cavity length (1.04 m), τ the measured cavity ring-down time with photolysis laser light, c the velocity of light, N and σ are the concentration and absorption cross section of the species of interest, respectively. Each ring-down trace was digitized with a time resolution of 20 ns. The digitized traces were transferred to a personal computer and averaged over 32 or 64 runs to calculate the ring-down rate, τ^{-1}. The validity of using of CRDS for kinetic studies derives from the fact that the lifetimes of the products generated by photolysis are much longer than the associated CRD times.[29]

To determine the initial Cl atom concentration, $[Cl]_0$, the production of ClO was measured at 266 nm using $Cl_2/O_3/O_2$ mixtures with photolysis of Cl_2 at 355 nm and $[Cl_2] = (1–10) \times 10^{15}$ molecule cm^{-3}.[30] Cl atoms are converted quantitatively into ClO radicals via $Cl + O_3 \rightarrow ClO + O_2$. O_3 was produced by irradiating an oxygen gas flow (slightly higher than 760 Torr (1 Torr = 133.322 Pa)) with a low-pressure Hg lamp (Hamamatsu Photonics, L937-02). The initial Cl atom concentration, $[Cl]_0$, using the absorption cross-section of ClO at 266 nm,[31] was observed to increase linearly with $[Cl_2]$.[30] $[Cl]_0$ was determined to be in the range of $(0.5–30) \times 10^{11}$ molecule cm^{-3}.

Sample gases for CH_3I and Cl_2 were prepared in glass gas bulbs with N_2 diluent. Then, the mixture gas was injected into a glass reaction cell. The gas flows were controlled by mass flow controllers (STEC, SEC-E40). The 355 nm output of a Nd^{3+}:YAG laser (Spectra Physics, GCR-250) was used to dissociate Cl_2. The typical dissociation laser intensity was (20 ± 2) or (100 ± 10) mJ $pulse^{-1}$. The IO radical concentration was monitored with an OPO laser (Spectra-Physics, MOPO-SL, spectral resolution 0.2 cm^{-1}) at 435.63 nm, the band head of the $A^2\Pi_{3/2} \leftarrow X^2\Pi_{3/2}$ ($v' = 3, v'' = 0$) transition.[32,33] The absorption cross-section of IO at 435.63 nm was previously measured to be 5.9×10^{-17} cm^2 $molecule^{-1}$ with the same spectral resolution.[34] The signal baseline was taken at 435.00 nm, a region in which there was no IO absorption. A large excess amount of O_2, 10^{14}–10^{18} molecule cm^{-3}, was used to maintain the pseudo-first-order reaction conditions. It is noted that no IO signal was observed after 532 nm irradiation of I_2/O_2 mixture at 298–338 K in 5–20 Torr total pressure of O_2 diluent, since I atom does not react with O_2. In addition, no formation of IO radical from the reaction $CH_3O_2 + I$ was reported.[17,35,36]

The reaction cell consisted of a Pyrex glass container (21 mm i.d.), which was evacuated by the combination of an oil rotary pump, a mechanical booster pump and a liq. N_2 trap. The temperature of the gas flow region was controlled over the range 278–338 K by circulation of water or ethanol with cooling circulators (EYELA, model NCB-2100, or THOMAS, model TRL-70SLP). The difference between the temperature of the sample gas at the entrance and exit of the flow region was measured to be <1 K. The pressure in the cell was monitored by an absolute pressure gauge (Baratron, 622A). A slow flow of nitrogen gas was introduced at the ends of the ring-down cavity, close to the mirrors, in order to minimize deterioration caused by exposure to the reactants and the products in the cell. The total flow rate was adjusted (typically 500 sccm) so that the gas in the cell was replaced completely within the 0.5 s time intervals between photolysis laser pulses. We experimentally confirmed that no difference of k_2 value in the change of the total N_2 flow rates from 200 sccm to 2000 sccm was observed. Hence, we can exclude the possibility that the gas generated by photolysis was accumulated in the cell. All reagents were obtained from commercial sources. CH_3I was obtained from Sigma Aldrich (>99%) and was subjected to freeze–pump–thaw cycling before use. The gas was premixed with N_2 diluent was prepared in a 10-liter Pyrex grass container. Cl_2 (>99.999%, Japan Air Liquid), N_2 (>99.999%, Teisan) and O_2 (>99.995%, Teisan) were used without further purification.

Results and Discussion

Mechanism of the Reaction of $CH_3I + Cl$ in the Presence of O_2. Rate constants were measured under the experimental conditions that CH_2I was generated by the abstraction reaction of CH_3I with Cl via reactions 6 and 7a. First, the following H-atom abstract and adduct formation reactions were investigated.

$$Cl_2 + h\nu(355\,nm) \rightarrow 2Cl \quad (6)$$

$$CH_3I + Cl \rightarrow CH_2I + HCl \quad (7a)$$

$$CH_3I + Cl + M \rightarrow CH_3I\text{–}Cl + M \quad (7b)$$

$$CH_3I\text{–}Cl + M \rightarrow CH_3I + Cl + M \quad (7c)$$

The CH_3I–Cl adduct was produced via reaction 7b and decayed mainly via the reverse reaction 7c, H-atom abstraction reaction 7a and diffusion loss.[37,38] A typical adduct decay profile is shown in Figure 1. Adduct temporal profiles were measured under the following experimental conditions; $Cl_2/CH_3I/O_2$ mixtures in 10 Torr N_2 diluent at 298 K, $[CH_3I] = 8.1 \times 10^{15}$ molecule cm^{-3}, $[Cl_2] = (5.7–8.5) \times 10^{14}$ molecule cm^{-3} and $[O_2] = (0.16–2.3) \times 10^{15}$ molecule cm^{-3}. Under these conditions, reaction 2 should proceed to completion within 0.3 to 4.2 ms. The adduct concentrations were derived from reported absorption cross-sections.[37]

The IBM Chemical Kinetics Simulator program was used to model the adduct formation profile as shown in Figure 1. $k_{7a} = 9.0 \times 10^{-13}$ cm^3 $molecule^{-1}$ s^{-1} was taken from a report by Bilde and Wallington.[39] k_{7b} and k_{7c} were taken from work by Ayhens et al.[38] Using these kinetic values, we estimated the pressure dependent rate constants by fitting to the following equations; $k_{7b} = [M]/(3.3 \times 10^{29} + 2.4 \times 10^{10}[M])$ and $k_{7c} = [M]/(9.1 \times 10^{14} + 6.8 \times 10^{-5}[M])$ in units of cm^3 $molecule^{-1}$ s^{-1} and s^{-1}, respectively, where [M] is the total gas concentration given in units of molecule cm^{-3} (Table 1). Other reactions are also included as shown in Table 1, e.g. reaction 8.[40]

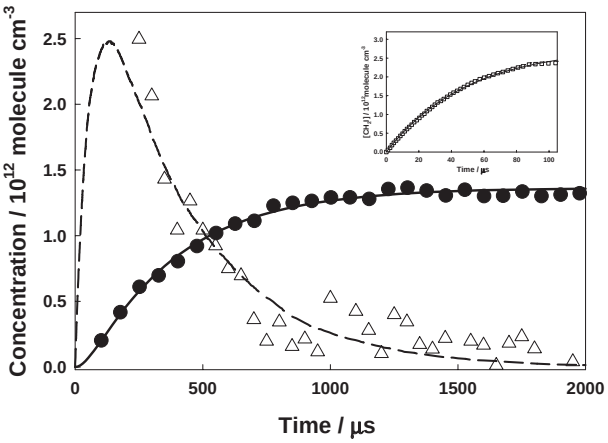

Figure 1. Rise and decay time-dependent profiles of CH_3I–Cl adduct and IO radical from the 355 nm photolysis of the mixture of Cl_2, CH_3I, and O_2 in 10 Torr N_2 diluent, where $[Cl_2] = 5.7 \times 10^{14}$, $[CH_3I] = 8.1 \times 10^{15}$, and $[O_2] = 1.1 \times 10^{15}$ molecule cm^{-3}. Triangle: [adduct], circle: [IO], smooth curve: fitting curve for IO with eq 11, broken curve: simulation for the adduct (Table 1). The IO temporal profile was obtained by subtraction of the absorption due to the CH_3ICl-adduct from the total absorption. The inset shows the simulated temporal profile, $[CH_2I]_t$, with squares, and a fitting curve to eq 9 with the solid curve.

$$CH_3I + CH_3I\text{–}Cl \rightarrow CH_3Cl + \text{products} \quad (8)$$

If we assume that reaction 8 is pressure-independent, the CH_3I–Cl time profiles are not fitted well by changing the total pressure. A similar reaction, $CH_3I + Cl$, is known to be pressure-dependent,[37–40] then the reaction 8 may proceed through an intermediate complex, too. Although this reaction is negligible at 10 Torr total pressure, we could assume that the rate constant is linearly dependent on the total pressure, $k_8 = 3.3 \times 10^{-32}$[M] cm^3 molecule^{-1} s^{-1} in order to determine the IO yields as described below. The observed adduct decay that starts from ≈300 μs is independent of the initial CH_3I concentrations, $[CH_3I] = (0.32–1.3) \times 10^{16}$ molecule cm^{-3} under 10 Torr total pressure condition.

The kinetic simulation results reproduce the experimental results well for adduct loss as shown by the broken curve in Figure 1. The diffusion loss rates of IO and CH_3I–Cl in Table 1 are defined by the fact that the radicals escape from the overlapping region between the prove laser and the photolysis laser. Due to the small diameter of the probe laser, the values are much larger than a diffusion loss rate usually seen in typical flash photolysis method. We determined the values from several time-profiles of IO and CH_3I–Cl under the present condition. Those values are in reasonable agreement with the previously measured typical diffusion loss rates in our experimental setup.[17,34,37]

In order to check the possibility of secondary reactions, several supplemental experiments were performed on the mixtures of $Cl_2/CH_3I/O_2$ under 10 Torr N_2. Maximum IO concentrations, $[IO]_{max}$, were derived from a single exponential fitting to the IO temporal profiles. $[IO]_{max}$ was measured as a function of $[Cl_2]$ over the range of $(0.8–4.1) \times 10^{15}$ molecule cm^{-3}. $[IO]_{max}$ is observed to be linear-dependent on this parameter within 20% experimental error, suggesting that there are no appreciable secondary reactions, e.g. $CH_2I + Cl_2$. When $[IO]_{max}$ was measured as a function of laser intensity (27 to 110 mJ pulse^{-1}) at $[CH_3I] = 8.1 \times 10^{15}$, $[Cl_2] = 9.7 \times 10^{14}$ and $[O_2] = 1.0 \times 10^{15}$ molecule cm^{-3}, respectively. $[IO]_{max}$ increased linearly with laser intensity with 2% experimental error as shown in Figure 2, again suggesting no appreciable secondary reactions.

Reaction Rate Constants of $CH_2I + O_2$. CH_2I evolution profiles via reactions 6 and 7 were simulated under the experimental conditions of $Cl_2/CH_3I/O_2$ mixtures in 10 Torr N_2 diluent at 298 K, $[CH_3I] = 8.1 \times 10^{15}$ and $[Cl_2] = (5.7–8.5) \times 10^{14}$ molecule cm^{-3} using reaction rate constants listed in Table 1. The evolution curve may be approximated by a single-exponential rise curve with $k_{rise} = 7.3 \times 10^3$ s^{-1}, calculated from the reported rate constant[41] for $CH_3I + Cl \rightarrow CH_2I + HCl$ and the concentration of CH_3I in the absence of O_2.

$$[CH_2I]_t = A(1 - \exp(-k_{rise}t)) \quad (9)$$

Under the presence of O_2, CH_2I reacts with O_2 to produce IO

Table 1. Reactions and Parameters at 298 K Used in Kinetic Simulations

Reaction		Rate constant[a)]	Reference
2	$CH_2I + O_2 \rightarrow$ products	1.28×10^{-12}	This work
7a	$CH_3I + Cl \rightarrow CH_2I + HCl$	9.0×10^{-13}	39
7b	$CH_3I + Cl + M \rightarrow CH_3I\text{–}Cl + M$	$[M]/(3.3 \times 10^{29} + 2.4 \times 10^{10}[M])$	38
7c	$CH_3I\text{–}Cl + M \rightarrow CH_3I + Cl + M$	$[M]/(9.1 \times 10^{14} + 6.8 \times 10^{-5}[M])$	38
8	$CH_3I + CH_3I\text{–}Cl + M \rightarrow$ products + M	3.3×10^{-32}[M][b)]	40
7d	$CH_3I\text{–}Cl + M \rightarrow$ other products + M	8.9×10^{-18}[M][b)]	40
14	$IO + IO \rightarrow OIO + I$	3.8×10^{-11}	41, 42
	$IO + IO \rightarrow$ other products	6.1×10^{-11}	41, 42
15	$I + IO \rightarrow I_2O$	2.2×10^{-12} [c)]	42
16	$I + I + M \rightarrow I_2 + M$	1.0×10^{-32}	43
17	Diffusion loss of CH_3I–Cl	2500[b)]	This work
18	Diffusion loss of IO	700[b)]	This work

a) In units of cm^6 molecule^{-2} s^{-1} or cm^3 molecule^{-1} s^{-1} or s^{-1}. b) See text for details. c) At 10 Torr total pressure of N_2.

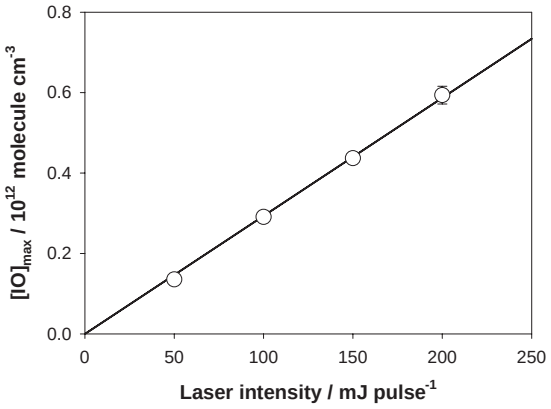

Figure 2. Laser intensity dependence of $[IO]_{max}$ at 10 Torr total N_2 pressure and 298 K, where $[CH_3I] = 8.1 \times 10^{15}$, $[Cl_2] = 9.7 \times 10^{14}$ and $[O_2] = 1.0 \times 10^{15}$ molecule cm^{-3}.

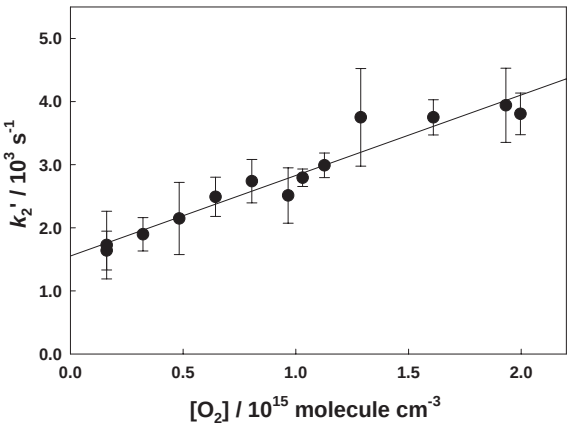

Figure 3. Second-order plots for the reaction of $CH_2I + O_2$ in 10 Torr N_2 diluent at 298 K.

via reaction 2. Therefore, the temporal profile of CH_2I should analytically follow eq 11 in the presence of O_2.

$$d[CH_2I]_t/dt = Ak_{rise}\exp(-k_{rise}t) - k_2'[CH_2I]_t \quad (10)$$

where $k_2' = k_2[O_2]$. Then, the temporal profile of IO radicals, $[IO]_t$, is analytically expressed by eq 11.

$$\begin{aligned}[IO]_t &= \phi_{IO}k'_2\int[CH_2I]_t dt \\ &= \phi_{IO}A\{k_{rise}(1-\exp(-k_2't)) \\ &\quad - k_2'(1-\exp(-k_{rise}t))\}/(k_{rise}-k_2') \end{aligned} \quad (11)$$

where ϕ_{IO} is the reaction branching ratio of the IO formation in reaction 2.

$$CH_2I + O_2 \rightarrow IO + HCHO \quad \phi_{IO} \quad (2b)$$

The value of ϕ_{IO} will be determined in the following section. The temporal profile of IO in the presence of O_2 was fitted using eq 11 as shown in Figure 1. Experiments were performed to obtain k_2' as a function of O_2 concentration over the range of $[O_2] = (0.16–2.3) \times 10^{15}$ molecule cm^{-3}. Figure 3 shows k_2' dependence on $[O_2]$ at 298 K, which gives $k_2 = (1.28 \pm 0.22) \times 10^{-12}$ cm^3 molecule^{-1} s^{-1} (the quoted uncertainty is 2σ). We experimentally determined values of k_2 to be independent from photolysis laser intensity over the range of 66–130 mJ pulse^{-1}, suggesting that the reaction mechanism does not contain reactions other than described above. Eskola et al. determined the rate constant k_2 to be 1.4×10^{-12} cm^3 molecule^{-1} s^{-1} at room temperature from the decay time profiles of CH_2I radical, which has no total He pressure dependence at $(0.2–15) \times 10^{17}$ molecule cm^{-3} and has a negative temperature dependence over the range of 220–450 K.[44] Masaki et al. also reported that the rate constant k_2 is $(1.6 \pm 0.2) \times 10^{-12}$ cm^3 molecule^{-1} s^{-1} and shows no total pressure dependence over the range of 2 to 15 Torr of N_2 diluent.[45]

In our previous work, which used the photodissociation of CH_2I_2 at 266 nm as a CH_2I radical source, we reported a k_2 value four-times smaller than we have observed here.[17] In the previous situation, the same concentrations of I atom and CH_2I radical were formed simultaneously from CH_2I_2 up to 10^{13} molecule cm^{-3}. One of the explanations to understand the discrepancy between the previous and present k_2 values could be that IO radical could be formed not only from the reaction $CH_2I + O_2$, but also from $CH_2IO_2 + I$ or other unknown I-atom concerned reactions in the previous condition. If one assumes that the formed CH_2IO_2 concentration was up to 5×10^{12} molecule cm^{-3} and the reaction rate constant with I atom was 1×10^{-10} cm^3 molecule^{-1} s^{-1} and the reaction of $CH_2IO_2 + I$ exclusively formed IO radicals, this secondary IO formation rate is estimated to be 500 s^{-1}. This value is $\approx$50% of IO formation from the direct reaction of CH_2I with O_2 at $[O_2] = 1 \times 10^{15}$ molecule cm^{-3},[17] hence this secondary reaction might affect the kinetics under previous condition. The reaction rate constant of $CH_2IO_2 + I$ was not reported yet, but the reaction of $CH_2IO_2 + I$ may produce CH_2IOOI adduct and may further react with I atom to reproduce CH_2IO_2 and molecular I_2 as reported in the case of the reaction of $CH_3O_2 + I$.[36] Another plausible explanation is that $CH_2IO_2^{\neq}$, an excited peroxy radical intermediate, may have a sufficient lifetime enough to slowly decompose and/or react with I atom to emit IO radical. Under the present conditions that utilizes Cl abstraction to generate CH_2I radicals without I atom generation, the secondary reactions did not interfere with present rate measurements since the concentration of I atom was sufficiently low.

We tested for the possibility of the participation of the $CH_2IO_2 + I \rightarrow CH_2IO + IO$ or $CH_2O_2 + I \rightarrow IO + HCHO$ reactions in the present reaction mechanism. Even if we assume the significantly high rate constant, $k = 1.0 \times 10^{-10}$ cm^3 molecule^{-1} s^{-1}, these IO formation mechanisms are not fast enough to reproduce the present IO rise time profiles in a model calculation under the present experimental conditions.

IO Yields from the Reaction of $CH_2I + O_2$ as a Function of N_2 Pressure. We have investigated the total IO yield, Y_{IO}, from reactions 2, 6, and 7 where Y_{IO} was estimated using the initial concentration of Cl atoms, $[Cl]_0$, and the total IO concentration. For determination of Y_{IO} in the mixture of $Cl_2/CH_3I/O_2$, we used much higher O_2 concentrations, $(5.6–8.1) \times 10^{16}$ molecule cm^{-3}, than that used in the kinetics experiments. Under such high O_2 concentration, reaction 2 proceeded to completion within 15 μs with the reaction rates much faster than any competing reactions. Since the decay of the IO signal was negligible (<1%) in this case, $[IO]_{total}$

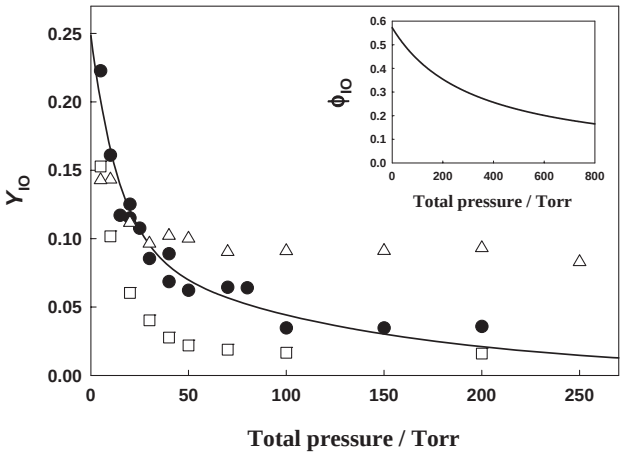

Figure 4. Pressure and temperature dependence of the yields of IO, Y_{IO}, in 2–3 Torr O_2 and 3–250 Torr N_2. Squares at 278 K, circles at 298 K, and triangles at 328 K. All Y_{IO} have errors estimated to be ≈30%. The simulation results in 298 K are shown by the solid curves. The inset shows the estimated reaction branching ratio, ϕ_{IO}, for IO formation from reaction 2b, which is given by eq 13. See text for details.

is approximated as $[IO]_{max}$:

$$[IO]_{total} = \phi_{IO}[CH_2I]_0$$
$$Y_{IO} = [IO]_{total}/[Cl]_0 \approx [IO]_{max}/[Cl]_0 \quad (12)$$

where Y_{IO} is the IO radical yield from the reaction of CH_3I with Cl atom in the presence of O_2 and ϕ_{IO} is the reaction branching ratio of the IO formation in reaction 2.

Figure 4 shows the total pressure and temperature dependence of Y_{IO} at 278, 298, and 328 K and for 5 to 250 Torr of N_2 diluent. The observed temperature dependence of Y_{IO} may be explained if CH_2IO_2 complex is thermally stabilized at the lower temperature, based on the present theoretical calculation as described below. In addition, the unknown temperature-dependent reactions of CH_3I–Cl, e.g. CH_3I–Cl + CH_3I–Cl, may play a role since CH_3I–Cl formation becomes more preferable than H-atom abstraction at lower temperature.[37,38] ϕ_{IO} was estimated at 298 K as follows, including the effect of adduct concern reactions, e.g. reaction 8, on Y_{IO} using kinetic simulations with the reaction rate constants shown in Table 1.

As for the reaction of CH_2I with O_2, Eskola et al. proposed the following excited peroxy radical formation mechanisms 2′ and 2′a–2′d.[44]

$$CH_2I + O_2 \rightarrow CH_2IO_2^{\neq} \quad (2')$$
$$CH_2IO_2^{\neq} + M \rightarrow CH_2IO_2 + M \quad (2'a)$$
$$CH_2IO_2^{\neq} \rightarrow IO + HCHO \quad (2'b)$$
$$CH_2IO_2^{\neq} \rightarrow CH_2O_2 + I \quad (2'c)$$
$$CH_2IO_2^{\neq} \rightarrow \text{other products} \quad (2'd)$$

where $CH_2IO_2^{\neq}$ stands for an excited intermediate species. ϕ_{IO} will be described as following.

$$\phi_{IO} = k_{2'b}/(k_{2'a}[M] + k_{2'b} + k_{2'c} + k_{2'd}) \quad (13)$$

Considering the mechanism above, the total pressure dependence of ϕ_{IO} (and Y_{IO}) was reproduced with the following ratios of rate constants $k_{2'a}/k_{2'b} = (1.7 \pm 0.9) \times 10^{-19}$ molecule^{-1} cm^3 and $(k_{2'c} + k_{2'd})/k_{2'b} = 0.75 \pm 0.02$. The simulation results for 298 K are given in Figure 4 by the solid curve. The pressure dependence of ϕ_{IO} is shown in the inset of Figure 4, which gives 0.17 ± 0.12 (2σ uncertainty) at 760 Torr. The other error would come from the estimate of $[Cl]_0$ by 19%. In addition, we can not exclude the possibility that the observed pressure dependence of Y_{IO} comes from unknown CH_3I–Cl loss reactions, e.g. CH_3I–Cl + IO. In this case, the present determined value 0.17 ± 0.12 at 760 Torr will be a lower limit value.

The contribution of non-IO reaction products, e.g. CH_2IO_2, on the present reaction mechanism was estimated using chemical simulations. We assumed that the branching ratio for CH_2IO_2 formation was 0.5 and the reaction rate constant of IO + CH_2IO_2 was 7.0×10^{-11} cm^3 molecule^{-1} s^{-1}.[46] Even so, the effect of the secondary reaction of IO + CH_2IO_2 on the values of k_2 and Y_{IO} were estimated to be <2% and <6%, respectively, under the present experimental conditions. The possibility that OH formation from the reaction of CH_2I with O_2 plays a role on the present kinetics and product yield studies was also checked. The reaction rate constant of CH_3I + OH is relatively low, 7.4×10^{-14} cm^3 molecule^{-1} s^{-1} at 298 K,[41] hence the effect will be negligible in the present experiment. This assumption was revealed to be reasonable by the observation that changing the initial concentration of CH_3I does not affect on the k_2 value. Using the chemical kinetics simulation we also confirmed that there are no significant effects on IO kinetics and yields even if we assumed the OH yield from the reaction of CH_2I + O_2 is 0.6. Hence, we conclude that non-IO products will not affect the results under the present experimental conditions. The fact that the product branching ratio is pressure dependent while the reported total rate constant is not pressure dependent is similar to the mechanism reported for the reaction of C_2H_3 + O_2.[47]

Theoretical calculations have been performed in order to obtain information on the reaction mechanism. All theoretical calculations were carried out using the Gaussian 03 Revision B.04 program package.[48] Details of the theoretical calculations were described previously.[37] The calculated energy diagram for CH_2I + O_2 is shown in Figure 5. According to the potential energy surfaces, the oxygen molecule attacks the carbon atom of CH_2I and the CH_2IO_2 complex is formed at the entrance region of the reaction without surmounting an energy barrier. The intermediate complex CH_2IO_2 structure is shown in Figure 6. No pressure dependence of the total reaction rate constant would be governed by the potential energy surface of the entrance region. IO is produced from this peroxy radical through deep well and a four-membered transition state (TS).[18] At higher pressures, because CH_2IO_2 is stabilized, the branching ratio of this reaction channel would have the pressure dependence. It should be emphasized that the transition state energy level is lower than that of the reactants CH_2I and O_2. These results support the direct formation of the IO radical from the reaction of CH_2I with O_2. In order to confirm the present calculation results, the energy diagram of the reaction of CH_2Br with O_2 has been calculated. Figure 7

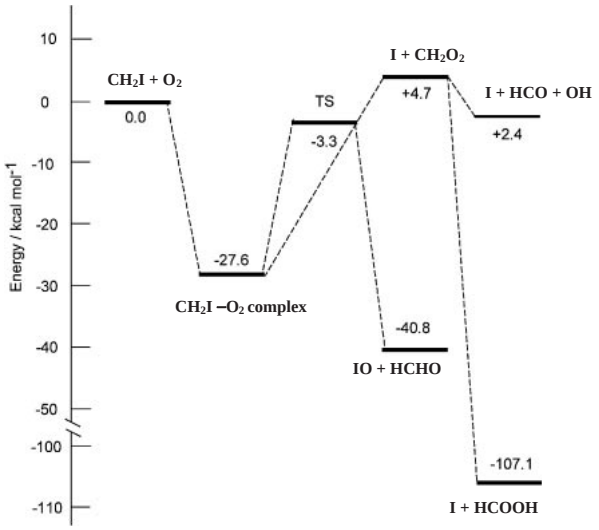

Figure 5. Calculated energy diagrams of the reactions of CH_2I with O_2. The value means relative energies/ kcal mol^{-1} (1 kcal mol^{-1} = 4.184 kJ mol^{-1}) with respect to the initial state ($CH_2I + O_2$) at the B3LYP/[6-311++ G(d,p),6-311G(d,p)] level.

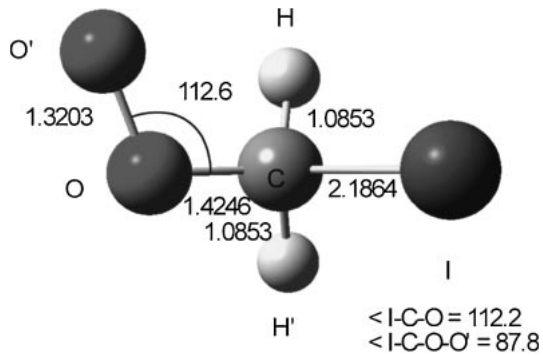

Figure 6. Optimized structures of the complex CH_2IO_2 in the reaction $CH_2I + O_2 \rightarrow IO + HCHO$ obtained at the B3LYP/[6-311++G(d,p),6-311G(d,p)] level. Bond lengths and angles are in Å and degrees, respectively.

shows considerably high transition state energy level to give BrO + HCHO. These theoretical results are consistent with the recent experimental observations that the reaction rate constant of $CH_2Br + O_2$ shows a typical third-body effect while that of $CH_2I + O_2$ shows no any total pressure effect.[44]

Eskola et al. detected I atom and IO radical from the reaction of $CH_2I + O_2$, using photoionization mass spectrometry.[44] They concluded that the I atom formation 2c is dominant and the IO radical formation 2b is minor pathway considering the upper limited sensitivity of HCHO detection.[44]

$$CH_2I + O_2 \rightarrow CH_2O_2 + I \qquad (2c)$$

However, the present theoretical calculations show that the $I + CH_2O_2$ formation pathway is endothermic as shown in Figure 5. Other I atom formation paths, e.g. I + HCO + OH and I + HCOOH, were investigated. We found that I + HCO + OH formation path is endothermic, hence this reaction path would not be important, either. We could not obtain transition states which produce I + HCOOH directly from

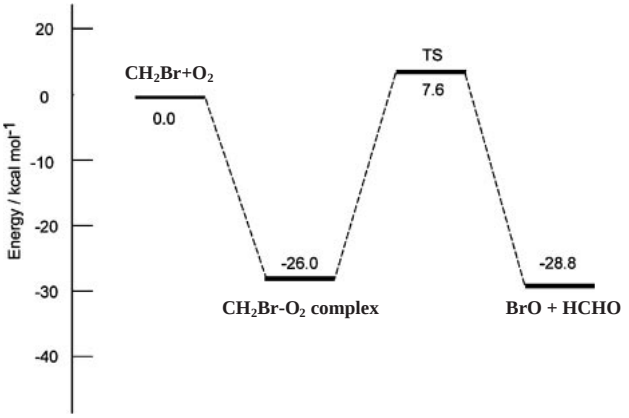

Figure 7. Calculated energy diagram of the reaction of CH_2Br with O_2 at the B3LYP/[6-311++G(d,p), 6-311G(d,p)] level. The value means relative energies/ kcal mol^{-1} with respect to the initial state ($CH_2Br + O_2$).

CH_2IO_2 intermediate. IUPAC subcommittee for gas kinetic evaluation reports that HCOOH formation from CH_2O_2 Criegee intermediate is estimated to zero.[41] However, Stefanopoulos et al. recently reported that the primary products from the reaction of $CH_2I/CHI_2 + O_2$ are HCHO and HCOOH using the combination of a Knudsen reactor, electron-impact mass spectrometry and FT-IR, which implies that IO and I atom formations are main channels in this reaction.[24] They calculated the reaction enthalpy for the reaction of $CH_2I + O_2$ at the B3P86/aug-cc-p VTZ-PP level of theory.[24] The reaction enthalpy of I + HCOOH formation is more exothermic than that of IO + HCHO formation,[24] which is consistent with the present results. However, they did not calculate any transition state energy levels.[24] Here we present that the transition state energy level for IO + HCHO formation is lower than the reactants and $I + CH_2O_2$ formation is endothermic. However, very recently Dillon et al. reported $\phi_{IO} \leq 0.12$ of IO formation from direct reaction of $CH_2I + O_2$, and the reaction of CH_2O_2 + I would be responsible for the IO observation.[49]

Cotter et al. reported a study of the products of the Cl-atom-initiated oxidation of CH_3I carried out in synthetic air at atmospheric pressure and at room temperature using FT-IR and found the only product from these reactions to be HCHO.[50] They could not detect any other products such as CH_2IOH, CHIO, HI, HCOOH, and CH_2IOOH. Recently, Orlando et al. reported[40,51] that one of the major primary products in the reaction of Cl atom with CH_3CH_2I (or CF_3CH_2I) in the presence of O_2 in an environmental chamber/FT-IR system was CH_3CHO (or CF_3CHO). Their theoretical calculation also revealed that I atom and the Criegee intermediate formation path is endothermic,[51] which is in good agreement with the present theoretical study.

It is clear, however, more detail branching ratio studies, e.g. simultaneous monitoring of CH_2IO_2, I and IO, are necessary in order to reveal the whole reaction mechanisms.

Conclusion

We determined a rate constant of $(1.28 \pm 0.22) \times 10^{-12}$ cm^3 molecule^{-1} s^{-1} at 298 K (2σ uncertainty) for the reaction of CH_2I with O_2 using 355 nm laser irradiation of $Cl_2/CH_3I/$

O_2 by monitoring IO radical with cavity ring-down spectroscopy. The observed IO yields from the reaction of CH_3I with Cl atom in the presence of O_2 show temperature and pressure dependence. Our kinetic analysis and theoretical calculations support direct IO formation from the reaction of CH_2I with O_2 and reveal that the reaction of $CH_2I + O_2$ is quite different from that of $CH_2Br + O_2$.

The authors appreciate Dr. T. J. Dillon (Max Planck Institute), Prof. S. Tsuchiya, Mr. H. Chiba (Josai University), Mr. C. D. Vecitis (California Institute of Technology) for helpful discussions. S.E. thanks the JSPS Research Fellowship for Young Scientists.

References

1 R. von Glasow, P. J. Crutzen, in *Tropospheric Halogen Chemistry in Treatise on Geochemistry*, ed. by H. D. Holland, K. K. Turekian, **2007**.

2 J. G. Calvert, S. E. Lindberg, *Atmos. Environ.* **2004**, *38*, 5087.

3 A. Saiz-Lopez, J. M. C. Plane, *Geophys. Res. Lett.* **2004**, *31*, L04112.

4 L. J. Carpenter, *Chem. Rev.* **2003**, *103*, 4953.

5 B. Alicke, K. Hebestreit, J. Stutz, U. Platt, *Nature* **1999**, *397*, 572.

6 C. D. O'Dowd, J. L. Jimenez, R. Bahreini, R. C. Flagan, J. H. Seinfeld, K. Hämeri, L. Pirjola, M. Kulmala, T. Hoffmann, *Nature* **2002**, *417*, 632.

7 J. B. Burkholder, J. Curtius, A. R. Ravishankara, E. R. Lovejoy, *Atmos. Chem. Phys.* **2004**, *4*, 19.

8 G. McFiggans, H. Coe, R. Burgess, J. Allan, M. Cubison, M. R. Alfarra, R. Saunders, A. Saiz-Lopez, J. M. C. Plane, D. Wevill, L. Carpenter, A. R. Rickard, P. S. Monks, *Atmos. Chem. Phys.* **2004**, *4*, 701.

9 D. Davis, J. Crawford, S. Liu, S. McKeen, A. Bandy, D. Thornton, F. Rowland, D. Blake, *J. Geophys. Res.* **1996**, *101*, 2135.

10 S. Enami, C. D. Vecitis, J. Cheng, M. R. Hoffmann, A. J. Colussi, *J. Phys. Chem. A* **2007**, *111*, 8749.

11 L. J. Carpenter, G. Malin, F. C. Küpper, P. S. Liss, *Global Biogeochem. Cycles* **2000**, *14*, 1191.

12 F. C. Küpper, L. J. Carpenter, G. B. McFiggans, C. J. Palmer, T. J. Waite, E.-M. Boneberg, S. Woitsch, M. Weiller, R. Abela, D. Grolimund, P. Potin, A. Butler, G. W. Luther, III, P. M. H. Kroneck, W. Meyer-Klaucke, M. C. Feiters, *Proc. Natl. Acad. Sci. U.S.A.* **2008**, *105*, 6954.

13 C. Peters, S. Pechtl, J. Stutz, K. Hebestreit, G. Hönninger, K. G. Heumann, A. Schwarz, J. Winterlik, U. Platt, *Atmos. Chem. Phys.* **2005**, *5*, 3357.

14 C. W. Spicer, E. G. Chapman, B. J. Finlayson-Pitts, R. A. Plastridge, J. M. Hubbe, J. D. Fast, C. M. Berkowitz, *Nature* **1998**, *394*, 353.

15 E. S. N. Cotter, N. J. Booth, C. E. Canosa-Mas, D. J. Gray, D. E. Shallcross, R. P. Wayne, *Phys. Chem. Chem. Phys.* **2001**, *3*, 402.

16 J. Sehested, T. Ellermann, O. J. Nielsen, *Int. J. Chem. Kinet.* **1994**, *26*, 259.

17 S. Enami, J. Ueda, M. Goto, Y. Nakano, S. Aloisio, S. Hashimoto, M. Kawasaki, *J. Phys. Chem. A* **2004**, *108*, 6347.

18 S. Enami, T. Yamanaka, S. Hashimoto, M. Kawasaki, K. Tonokura, H. Tachikawa, *Chem. Phys. Lett.* **2007**, *445*, 152.

19 R. Wada, J. M. Beames, A. J. Orr-Ewing, *J. Atmos. Chem.* **2007**, *58*, 69.

20 A. Saiz-Lopez, A. S. Mahajan, R. A. Salmon, S. J. B. Bauguitte, A. E. Jones, H. K. Roscoe, J. M. C. Plane, *Science* **2007**, *317*, 348.

21 A. Saiz-Lopez, J. M. C. Plane, J. A. Shillito, *Geophys. Res. Lett.* **2004**, *31*, L03111.

22 Y. Nakano, T. Ishiwata, M. Kawasaki, *J. Phys. Chem. A* **2005**, *109*, 6527.

23 Y. Nakano, H. Ukeguchi, T. Ishiwata, *Chem. Phys. Lett.* **2006**, *430*, 235.

24 V. G. Stefanopoulos, V. C. Papadimitriou, Y. G. Lazarou, P. Papagiannakopoulos, *J. Phys. Chem. A* **2008**, *112*, 1526.

25 A. O'Keefe, D. A. G. Deacon, *Rev. Sci. Instrum.* **1988**, *59*, 2544.

26 M. D. Wheeler, S. M. Newman, A. J. Orr-Ewing, M. N. R. Ashfold, *J. Chem. Soc., Faraday Trans.* **1998**, *94*, 337.

27 T. Yu, M. C. Lin, *J. Phys. Chem.* **1995**, *99*, 8599.

28 S. Enami, Y. Hoshino, Y. Ito, S. Hashimoto, M. Kawasaki, T. J. Wallington *J. Phys. Chem. A* **2006**, *110*, 3546.

29 S. S. Brown, A. R. Ravishankara, H. J. Stark, *J. Phys. Chem. A* **2000**, *104*, 7044.

30 K. Suma, Y. Sumiyoshi, Y. Endo, S. Enami, S. Aloisio, S. Hashimoto, M. Kawasaki, S. Nishida, Y. Matsumi, *J. Phys. Chem. A* **2004**, *108*, 8096.

31 S. P. Sander, R. R. Friedl, D. M. Golden, M. J. Kurylo, G. K. Moortgat, P. H. Wine, A. R. Ravishankara, C. E. Kolb, M. J. Molina, B. J. Finlayson-Pitts, R. E. Huie, V. L. Orkin, *Chemical Kinetics and Photochemical Data for Use in Stratospheric Modeling; Evaluation 15*, Jet Propulsion Laboratory, Pasadena, CA, **2006**.

32 S. M. Newman, W. H. Howie, I. C. Lane, M. R. Upson, A. J. Orr-Ewing, *J. Chem. Soc., Faraday Trans.* **1998**, *94*, 2681.

33 P. Spietz, J. C. Gomez Martin, J. P. Burrows, *J. Photochem. Photobiol., A* **2005**, *176*, 50.

34 Y. Nakano, S. Enami, S. Nakamichi, S. Aloisio, S. Hashimoto, M. Kawasaki, *J. Phys. Chem. A* **2003**, *107*, 6381.

35 C. E. Canosa-Mas, A. Vipond, R. P. Wayne. *Phys. Chem. Chem. Phys.* **1999**, *1*, 761.

36 T. J. Dillon, M. E. Tucceri, J. N. Crowley, *Phys. Chem. Chem. Phys.* **2006**, *8*, 5185.

37 S. Enami, S. Hashimoto, M. Kawasaki, Y. Nakano, T. Ishiwata, K. Tonokura, T. J. Wallington, *J. Phys. Chem. A* **2005**, *109*, 1587.

38 Y. V. Ayhens, J. M. Nicovich, M. L. McKee, P. H. Wine, *J. Phys. Chem. A* **1997**, *101*, 9382.

39 M. Bilde, T. J. Wallington, *J. Phys. Chem. A* **1998**, *102*, 1550.

40 J. J. Orlando, C. A. Piety, J. M. Nicovich, M. L. Mckee, P. H. Wine, *J. Phys. Chem. A* **2005**, *109*, 6659.

41 R. Atkinson, D. L. Baulch, R. A. Cox, J. N. Crowley, R. F. Hampson, Jr., J. A. Kerr, M. J. Rossi, J. Troe, IUPAC Subcommittee on Gas Kinetic Data Evaluation for Atmospheric Chemistry Web Version, December, **2001**.

42 W. J. Bloss, D. M. Rowley, R. A. Cox, R. L. Jones, *J. Phys. Chem. A* **2001**, *105*, 7840.

43 M. E. Jenkin, R. A. Cox, A. Mellouki, G. Le Bras, G. Poulet, *J. Phys. Chem.* **1990**, *94*, 2927.

44 A. J. Eskola, D. Wojcik-Pastuszka, E. Ratajczak, R. S. Timonen, *Phys. Chem. Chem. Phys.* **2006**, *8*, 1416.

45 A. Masaki, S. Tsunashima, N. Washida, *J. Phys. Chem.* **1995**, *99*, 13126.

46 S. Enami, T. Yamanaka, S. Hashimoto, M. Kawasaki, Y. Nakano, T. Ishiwata, *J. Phys. Chem. A* **2006**, *110*, 9861.

47 A. M. Mebel, E. W. G. Diau, M. C. Lin, K. Morokuma, *J. Am. Chem. Soc.* **1996**, *118*, 9759.

48 M. J. Frisch, G. W. Trucks, H. B. Schlegel, G. E. Scuseria, M. A. Robb, J. R. Cheeseman, J. A. Montgomery, Jr., T. Vreven, K. N. Kudin, J. C. Burant, J. M. Millam, S. S. Iyengar, J. Tomasi, V. Barone, B. Mennucci, M. Cossi, G. Scalmani, N. Rega, G. A. Petersson, H. Nakatsuji, M. Hada, M. Ehara, K. Toyota, R. Fukuda, J. Hasegawa, M. Ishida, T. Nakajima, Y. Honda, O. Kitao, H. Nakai, M. Klene, X. Li, J. E. Knox, H. P. Hratchian, J. B. Cross, C. Adamo, J. Jaramillo, R. Gomperts, R. E. Stratmann, O. Yazyev, A. J. Austin, R. Cammi, C. Pomelli, J. W. Ochterski, P. Y. Ayala, K. Morokuma, G. A. Voth, P. Salvador, J. J. Dannenberg, V. G. Zakrzewski, S. Dapprich, A. D. Daniels, M. C. Strain, O. Farkas, D. K. Malick, A. D. Rabuck, K. Raghavachari, J. B. Foresman, J. V. Ortiz, Q. Cui, A. G. Baboul, S. Clifford, J. Cioslowski, B. B. Stefanov, G. Liu, A. Liashenko, P. Piskorz, I. Komaromi, R. L. Martin, D. J. Fox, T. Keith, M. A. Al-Laham, C. Y. Peng, A. Nanayakkara, M. Challacombe, P. M. W. Gill, B. Johnson, W. Chen, M. W. Wong, C. Gonzalez, J. A. Pople, *Gaussian 03, Revision B.04*, Gaussian, Inc., Pittsburgh, PA, **2003**.

49 T. J. Dillon, M. E. Tucceri, R. Sander, J. N. Crowley, *Phys. Chem. Chem. Phys.* **2008**, *10*, 1540.

50 E. S. N. Cotter, N. J. Booth, C. E. Canosa-Mas, R. P. Wayne, *Atmos. Environ.* **2001**, *35*, 2169.

51 J. Orlando, P. H. Wine, J. M. Nicovich, D. T. Huskey, J. E. Allen, C. A. Piety, M. L. McKee, T. J. Wallington, M. D. Hurley, M. S. Javadi, O. J. Nielsen, American Geophysics Union Fall Meeting, San Francisco, CA, USA, December 10–14, **2007**.